Chem. Mater. **1998,** *10,* 3475−3483

A New Role of the Surfactant in the Synthesis of Mesostructured Phases: Dodecyl Phosphate as Template and Reactant for Aluminophosphates

Michael Fröba* and Michael Tiemann

Institute of Inorganic and Applied Chemistry, University of Hamburg,
Martin-Luther-King-Platz 6, D-20146 Hamburg, Germany

Received April 9, 1998. Revised Manuscript Received July 26, 1998

Lamellar mesostructured aluminophosphates were synthesized from aluminum triisopropoxide and phosphoric acid; monododecyl phosphate surfactant was used as structure-directing template. Depending on the relative Al/P ratio in the samples, variable relative amounts of tetrahedrally and octahedrally coordinated Al are found, indicating that both aluminophosphate and aluminum oxide species (as thermodynamically favored) are being formed in the syntheses. This is investigated quantitatively by Al K-edge XANES spectroscopy. The same syntheses were carried out without phosphoric acid, resulting in similar lamellar structures. The inorganic lamellae of these products consist to a significant extent of aluminophosphate rather than exclusively of aluminum oxide, which means that the phosphate headgroups of the surfactant molecules become incorporated into the inorganic network. Thus, for the first time, the surfactant serves as both template and reactant.

Introduction

On account of the great catalytic potential of zeolite-analogous microstructured aluminophosphates ($AlPO_4$-*n*), first introduced in 1982 by Wilson et al.,[1] numerous attempts have been made to prepare mesostructured aluminophosphates following the synthetic route presented by researchers of Mobil Oil in 1992,[2] which utilizes supramolecular arrays of surfactants as structure-directing templates under hydrothermal conditions. The first hydrothermal synthesis of mesostructured aluminophosphates by liquid-crystal templating was performed by Sayari et al.,[3,4] who used primary alkylamines, such as $C_{12}H_{25}NH_2$, and tertiary dimethylalkylamines of comparable chain lengths as surfactants; in contrast, M41S silica phases are commonly prepared using cationic surfactants. Catapal B alumina and H_3PO_4 served as inorganic precursors and crystallization was carried out at 373 K for 24 h. In this synthesis the surfactant molecules are protonated both during the reaction (the pH of the gel is around 3) and in the final solid product, as was shown by ^{15}N and ^{13}C NMR spectroscopy. The products were lamellar mesostructures, as evidenced by powder XRD and TEM; accordingly, the surfactant could not be removed by calcination without collapse of the structure. Both the variation of the Al/P ratio and of the surfactant/P ratio resulted in the formation of different lamellar phases with *d* spacings between 2.2 and 3.6 nm (for dodecylamine); even in the absence of aluminum, a mesostructure was obtained, whereas a phosphorus-free synthesis led to amorphous material. Depending on the Al/P ratio, ^{27}Al NMR revealed different relative amounts of tetrahedrally and octahedrally coordinated aluminum, the latter being attributed to coordination with four PO_4 groups and two water molecules and to unreacted educt. ^{31}P NMR spectroscopy revealed different forms of phosphorus coordination and showed the absence of P−O−P coordination.

Sayari et al. also found a structural feature in aluminophosphates that was previously not observed among mesostructured phases.[5] TEM pictures show coaxial cylindrical layers, where the XRD pattern is the same as that of a sample with a planar lamellar structure. The fact that the growth of these curved layers seems to originate from the center indicates the presence of rodlike micelles; thus, the formation of layered material rather than hexagonal seems to be favored.

Prior to the work mentioned above, Ozin et al.[6−8] prepared lamellar aluminophosphates under solvothermal conditions using primary alkylamines in tetraethylene glycol. However, their work focused mainly on SEM investigations of the morphology of the samples, which revealed remarkable similarities to natural biomineralogical structures.

Mesostructured aluminophosphates could also be obtained by nonsolvothermal synthesis using cationic

---

(1) Wilson, S. T.; Lok, B. 1M.; Messina, C. A.; Cannan, T. R.; Flanigen, E. M. *J. Am. Chem. Soc.* **1982**, *104*, 1146.

(2) Beck, J. S.; Vartuli, J. C.; Roth, W. J.; Leonowicz, M. E.; Kresge, C. T.; Schmitt, K. D.; Chu, C. T−W.; Oloson, D. H.; Sheppard, E. W.; McCullen, S. B.; Higgins, J. B.; Schlenker, J. L. *J. Am. Chem. Soc.* **1992**, *114*, 10834

(3) Sayari, A.; Karra, V. R.; Reddy, J. S.; Moudrakovski, I. *Chem. Commun.* **1996**, 411

(4) Sayari, A.; Moudrakovski, I.; Reddy, J. S.; Ratcliffe, C. I.; Ripmeester, J. A.; Preston, K. F. *Chem. Mater.* **1996**, *8*, 2080

(5) Sayari, A.; Karra, V. R.; Reddy, J. S.; Moudrakovski, I. *Chem. Commun.* **1996**, 413

(6) Oliver, S.; Kuperman, A.; Coombs, N.; Lough, A.; Ozin, G. A. *Nature* **1995**, *378*, 47

(7) Oliver, S.; Coombs, N.; Ozin, G. A. *Adv. Mater.* **1995**, *7*, 931

(8) Ozin, G. A.; Oliver, S. *Adv. Mater.* **1995**, *7*, 943

10.1021/cm980712c CCC: $15.00

surfactants. Stucky et al.[9] prepared a hexagonal phase (as proven by XRD and TEM) by adding a solution of H_3PO_4 and HF to aluminum isopropoxide in ethanol; after the addition of cetyltrimethylammonium bromide (CTABr) the pH was adjusted to ca. 8 using tetramethylammonium hydroxide, followed by stirring at room temperature for 4 h. The product undergoes a transformation to a lamellar phase at 70 °C. Fluoride is found to be part of the final product (by elemental analysis), and ^{27}Al NMR spectra show both tetrahedral and octahedral coordination of aluminum in the hexagonal phase, whereas the tetrahedral coordination is predominant in the lamellar phase.

By a similar approach, Kevan et al.[10] obtained a thermally stable hexagonal aluminophosphate using cetyltrimethylammonium chloride (CTACl) as surfactant and $Al(OH)_3$ as aluminum source. The template is removed upon calcination, giving a porous material with a surface area of 770 m^2/g.

In summary, mesostructured aluminophosphates were synthesized using both nonionic and cationic surfactants as templating agents. Anionic surfactants have played only a minor role in the synthesis of aluminophosphates so far. Stucky et al.[11] used sodium salts of dodecyl phosphate as templating species for mesostructured compounds of aluminum and zinc, suggesting that in some cases the phosphate groups get incorporated into the framework, since no sodium is found in the final products. Ozin et al.[12] prepared a chemical composite of hydroxyapatite and lamellar calcium dodecyl phosphate; Yada et al.[13] synthesized phosphate-free aluminum-based mesostructured materials with lamellar and hexagonal structures using sodium dodecyl sulfate (SDS).

Experimental Section

The aluminophosphate samples were prepared by adding aluminum isopropoxide ($Al(O^iPr)_3$, Merck) and, in some cases, phosphoric acid (H_3PO_4, Merck) to an aqueous solution of monododecyl phosphate ($C_{12}H_{25}OPO(OH)_2$, Lancaster). The mixture was stirred at room temperature for 1 h, transferred into a Teflon-lined autoclave, and kept at 393 K for 24 h without agitation. The product was filtered off, washed with ethanol, and dried in a vacuum. The concentration of the surfactant was varied. Different relative amounts of $Al(O^iPr)_3$, H_3PO_4, and surfactant were used.

Powder X-ray diffraction (XRD) was performed on a Philips PW 1050/25 diffractometer using filtered Cu Kα radiation. In situ temperature-resolved powder X-ray diffraction was carried out using a Philips low-temperature chamber mounted on a PW 3020 goniometer. Transmission electron microscopy (TEM) was carried out with a Philips STEM 400 electron microscope. Simultaneous thermogravimetry (TG), differential thermal analysis (DTA), and mass spectrometry (MS) were performed on a Netzsch STA 409 thermobalance and a Baltzer QMG 421 quadrupole mass spectrometer coupled by a Baltzer 403/4 capillary coupling system (multiple ion detection method); samples were heated at 5 K/min in an open alumina crucible at normal pressure under dynamic air atmosphere. X-ray absorption (XANES) spectra at the Al K-edge were recorded at the JUMBO 3-3 beamline at Stanford Synchrotron Radiation Laboratory (SSRL at SLAC), Stanford, CA, at room temperature in total electron yield mode. The SPEAR electron storage ring was running at 3 GeV with a current of ca. 60−95 mA. The beamline was equipped with a YB_{66} (400) double-crystal monochromator.[14,15] The spectra were calibrated against the edge position of pure aluminum (1559 eV), preedge fitted and normalized with WINXAS software.[16]

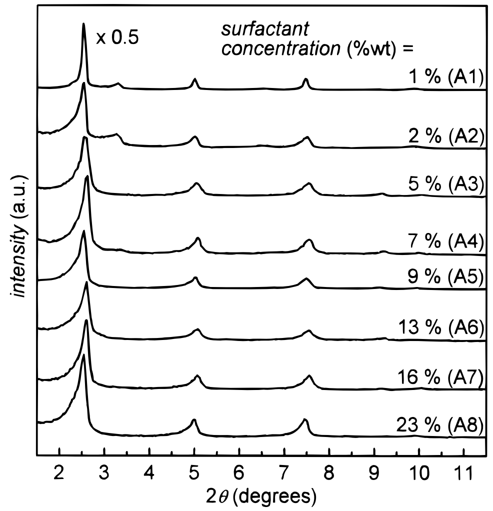

Figure 1. XRD patterns of samples prepared by method A with equal amounts of $Al(O^iPr)_3$, H_3PO_4, and $C_{12}-PO_4$ surfactant.

Results and Discussion

Powder XRD, Transmission Electron Microscopy, and Elemental Analysis. Mesostructured aluminophosphates were synthesized from equal amounts of aluminum triisopropoxide ($Al(O^iPr)_3$), phosphoric acid (H_3PO_4), and monododecyl phosphate ($C_{12}H_{25}OPO(OH)_2$, in the following noted as $C_{12}-PO_4$). Different amounts of water were used to vary the surfactant concentration over the range 1−23 wt % (0.05−1.11 mol/L). The powder XRD patterns (Figure 1) of these products are similar to each other and consist of one set of equidistant reflections which may be explained as 00*l* reflections of a single lamellar phase with a *d* spacing of ca. 3.55 nm; in some cases an additional set of equidistant reflections of low intensity, corresponding to a weak second lamellar phase (*d* spacing ca. 2.69 nm), is observed (see Table 1). Figure 2 shows a transmission electron micrograph of the sample A3 prepared with a surfactant concentration of 5 wt % ; the striped pattern is consistent with the lamellar structure.

The same syntheses were carried out without H_3PO_4 as a phosphorus source. In these cases the only phosphate groups available in the reaction mixture are those from the surfactant. In the following, the synthetic method in which H_3PO_4 is used will be referred to as method A and the synthesis without H_3PO_4 will

---

[9] Feng, P.; Xia, Y.; Feng, J.; Bu, X.; Stucky, G. *Chem. Commun.* **1997**, 949

[10] Zhao, D.; Luan, Z.; Kevan, L. *Chem. Commun.* **1997**, 1009

[11] Huo, Q.; Margolese, D. I.; Ciesla, U.; Feng, P.; Gier, T. E.; Sieger, P.; Leon, R.; Petroff, P. M.; Schüth, F.; Stucky, G. D. *Nature* **1994**, *368*, 317

[12] Ozin, G. A.; Varaksa, N.; Coombs, N.; Davies, J. E.; Perovic, D. D., Ziliox, M. *J. Mater. Chem.* **1997**, 1601

[13] Yada, M.; Kitamura, H.; Machida, M.; Kijima, T. *Langmuir* **1997**, *13*, 5252

[14] Wong, J.; George, G.; Pickering, I.; Rek, Z.; Rowen, M.; Tanaka, T.; Via, G.; Brown, G. E., Jr. *Solid State Comm.* **1994**, *92*, 559

[15] Wong, J.; Shimkaveg, G.; Goldstein, W.; Eckart, M.; Tanaka, T.; Rek, Z. U.; Tompkins, H. *Nucl. Instr. Methods* **1990**, *A291*, 243

[16] Ressler, T. *J. Synchrotron Rad.* **1998**, *5*, 118

Table 1. Synthesis Parameters and *d* Spacings (minor phases in parentheses) of Samples Prepared from Equal Amounts of Al(O^{i}Pr)$_3$, H_3PO_4, and C_{12}−PO_4 Surfactant

surfactant concn		synthesis with H_3PO_4			synthesis without H_3PO_4		
wt %	mol/L	no.	*d* (nm)		no.	*d* (nm)	
1	0.05	A1	3.55	(2.68)	B1		2.71
2	0.09	A2	3.54	(2.69)	B2		2.71
5	0.18	A3	3.52		B3		2.69
7	0.28	A4	3.52		B4		2.71
9	0.37	A5	3.56		B5	(3.58)	2.70
13	0.55	A6	3.52		B6	3.55	(2.70)
16	0.74	A7	3.52		B7	3.54	(2.69)
23	1.11	A8	3.55		B8	3.55	(2.69)

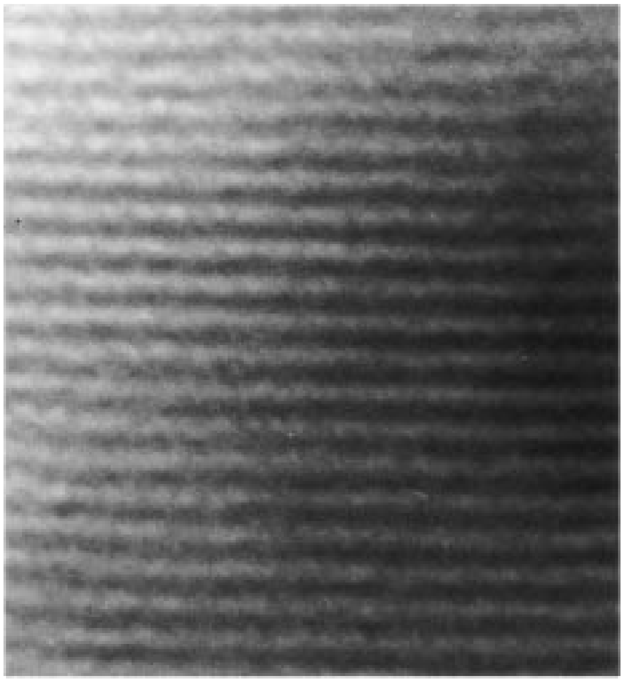

Figure 2. Transmission electron micrograph of the sample A3.

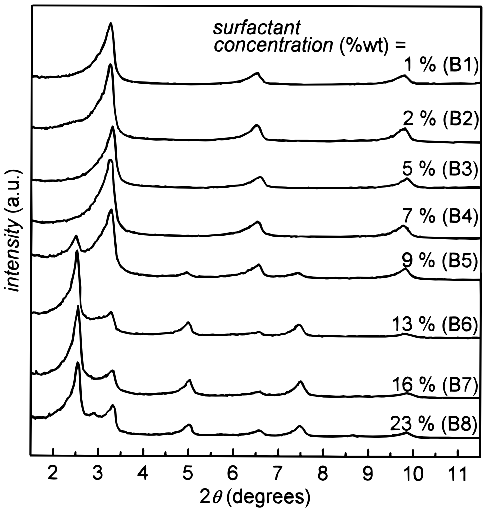

Figure 3. XRD patterns of samples prepared by method B with equal amounts of Al(O^{i}Pr)$_3$ and C_{12}−PO_4 surfactant.

Table 2. Synthesis Parameters, Elemental Analysis and *d* Spacings (minor phases in parentheses) of Samples Prepared with Different Amounts of Al(O^{i}Pr)$_3$, H_3PO_4, and C_{12}-PO_4 Surfactant

		analytical molar ratios				
no.	input ratio[a]	C/P	Al/P	ratio[b] calcd from anal.	*d* (nm) 1st and 2nd phase	
A9	0.5/1/1	10.70	0.45	0.51/0.12/1		3.53
A10	1/1/1	4.86	0.79	1.88/1.37/1		3.52
A11	1.5/1/1	4.40	0.83	2.26/1.73/1		3.49
A12	2/1/1	5.77	0.88	2.01/1.27/1	2.68	(3.44)
A13	3/1/1	5.29	1.24	2.59/1.08/1	2.71	(3.65)
A14	8/1/1	5.06	3.36	8.29/1.47/1	2.69	
B9	0.25/0/1	11.84	0.46		(2.67)	3.56
B10	0.5/0/1	12.70	0.55			3.56
B11	1/0/1	11.50	1.11		(2.70)	3.55
B12	1.25/0/1	11.65	1.30		(2.71)	3.56
B13	1.5/0/1	12.23	1.51		2.73	
B14	2/0/1	12.05	1.78		2.72	(3.51)
B15	4/0/1	12.02	3.93		2.73	

[a] Al(O^{i}Pr)$_3$/H_3PO_4/C_{12}−PO_4 ratio. [b] Al/$P_{H_3PO_4}$/$P_{C_{12}-PO_4}$ ratio.

be denoted as method B. For low surfactant concentrations, the XRD patterns of these method B products (Figure 3) indicate a single lamellar phase with a *d* spacing of ca. 2.70 nm; a second lamellar phase with a *d* spacing of ca. 3.55 nm occurs and becomes predominant when the surfactant concentration is increased (see Table 1).

Finally, syntheses with a constant surfactant concentration of 13 wt % and variable amounts of Al(O^{i}Pr)$_3$ and H_3PO_4 relative to the amount of the surfactant were carried out. Again, the same syntheses were repeated without any H_3PO_4.

Information on the molar compositions of the samples is obtained from C, Al, and P elemental analysis. The relative ratios of the elements in the samples are to be compared to the relative ratios of the reactants used for the preparations. Particular interest lies in the amount of P and its origin, since in those products that are synthesized by method A, two different P sources contribute to the final overall P content. Table 2 shows the relative Al/P and C/P ratios in the products as found by elemental analysis compared to the relative amounts of Al(O^{i}Pr)$_3$, H_3PO_4, and surfactant originally used for the syntheses. The Al/P ratios found by analysis are greater than expected if the theoretical value is low and smaller than expected if the theoretical value is great, the latter being the case especially for samples prepared with H_3PO_4 (method A). For the samples prepared without H_3PO_4 (method B) the C/P ratio fits in with the expected one $C/P = 12$ (with a deviation averaging ca. 2.5%). Accordingly, for those samples which were prepared with H_3PO_4 (method A), the relative contributions of P from H_3PO_4 and P from the surfactant to the overall amount of P can be calculated by $P_{H_3PO_4}/P_{\mathrm{surfactant}} = 12/(C/P) - 1$. The XRD patterns of the products prepared with (Figure 4) and without H_3PO_4 (Figure 5) show two sets of equidistant reflections, corresponding to two lamellar phases with *d* spacings of ca. 2.70 and 3.55 nm, respectively, with variable relative intensities in dependence on the Al/P ratio (see below).

Both types of syntheses (methods A and B) led to X-ray amorphous materials when no surfactant or no Al(O^{i}Pr)$_3$ were used; when both H_3PO_4 and the surfactant were absent in the reaction mixture, the product could be identified by powder XRD as γ-AlO(OH) (boehmite).

The acidity of the surfactant is approximately the same as that of H_3PO_4; thus, the pH conditions of the syntheses with and without H_3PO_4 are quite similar (pH $\approx$ 2).

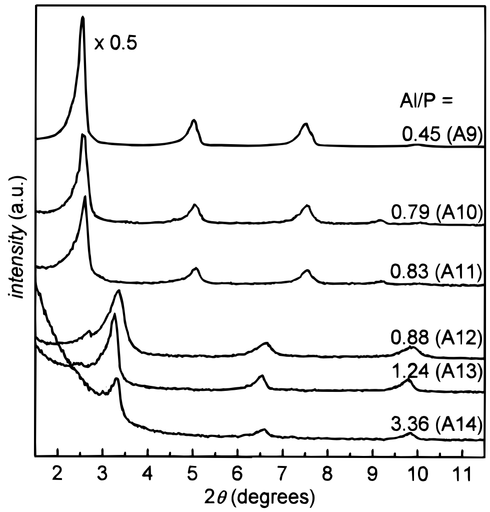

Figure 4. XRD patterns of samples prepared by method A with variable relative amounts of Al(O^{i}Pr)$_3$, H_3PO_4, and $C_{12}-PO_4$ surfactant (13wt %). The relative ratios Al to overall-P as found by elemental analysis are indicated.

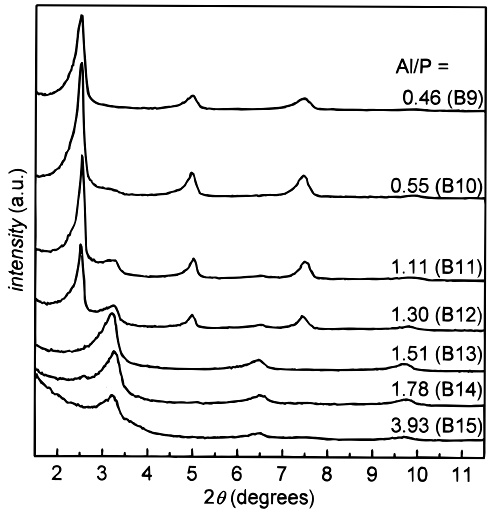

Figure 5. XRD patterns of samples prepared by method B with variable relative amounts of Al(O^{i}Pr)$_3$ and $C_{12}-PO_4$ surfactant (13wt %). The relative ratios Al/P as found by elemental analysis are indicated.

In conclusion, mesostructured materials prepared with H_3PO_4 consist almost exclusively of one lamellar phase with a large *d* spacing (3.55 nm) as long as Al and P are used in approximately the same relative amounts; no systematic dependence on the surfactant concentration is observed. Phases with smaller *d* spacings (2.69 nm) occur only when the Al/P ratio is increased. Even when no free phosphate ions from H_3PO_4 are available in the reaction mixture, lamellar mesostructured materials are obtained. For equal amounts of Al and P these phases have smaller *d* spacings than samples prepared with H_3PO_4, unless the surfactant concentration is very high; in that case, an additional phase with a large *d* spacing, equal to that of samples prepared with H_3PO_4, becomes predominant. The same trend is observed when the Al/P ratio is decreased.

In our opinion, there are two possible explanations for the occurrence of mesostructured materials from the syntheses free of H_3PO_4 (method B). The first is that the aluminum building units react with the phosphate groups of the surfactant molecules; the surfactant headgroups become part of the inorganic networks in the products. This explanation is strongly supported by the fact that smaller *d* spacings are observed in samples prepared without H_3PO_4 than in those prepared with H_3PO_4 (as long as the Al/P ratio is approximately 1 and the surfactant concentration is not too high): The double layer of the surfactant molecules between the inorganic lamellae is thinner, because the phosphate headgroups do not contribute, since they are inside and part of the layers themselves.

The possible formation of free phosphate ions by decomposition of the surfactant molecules can be excluded, since the latter is stable under hydrothermal conditions at a temperature of 393 K. After treating an aqueous solution of dodecyl phosphate under the same experimental conditions, the intact surfactant was recovered, as evidenced by powder XRD.

The other possible explanation for the formation of mesostructures in the method B syntheses is that no phosphate takes part in the condensation process at all and that the networks in the products consist of aluminum oxide or aluminum oxyhydroxide species, presumably γ-AlO(OH) (boehmite), which (as noted above) is formed in a synthesis free of both H_3PO_4 and the surfactant. (Boehmite is the thermodynamically favored aluminum oxide species under the conditions present in the syntheses.) However, this situation cannot be presumed for the products of the reactions with H_3PO_4 (method A); at least here, free phosphate ions definitely do react with the aluminum units, since more P is found by elemental analysis than may be accounted for by the surfactant headgroups. (The formation of an insoluble amorphous phosphorus species under these reaction conditions, which would lead to the same analytical result, is unlikely.) This proves that the thermodynamically most stable 6-fold coordination of Al with O is not the generally favored product of our syntheses; instead, Al definitely reacts with phosphate, leading to the formation of Al tetrahedrally coordinated with P over O-bridges. This is also apparent from Al K-edge XANES spectroscopy (see below) to be the case not only with free phosphate ions but also with the surfactant phosphate groups that are bonded to the alkyl chain. This means that the surfactant serves both as a template and as a reactant. In the following, this will be founded by further evidence.

Finally, the possible formation of pure aluminum oxide or oxyhydroxide outside the lamellae must be taken into consideration; the products could be mixtures of the mesostructured aluminophosphate phases and, additionally, aluminum oxide phases, either crystalline or amorphous. However the powder XRD patterns do not show the typical indications (broad reflections in the region $2\theta > 10°$) of significant amounts of amorphous material and no reflections of any crystalline material are found. Therefore, any oxide species present in the samples may be considered to be part of the mesostructures.

Al K-Edge XANES Spectroscopy. To distinguish between tetrahedral mesostructured aluminophosphate and octahedral aluminum oxide species the products were examined by X-ray absorption spectroscopy at the Al K-edge. From XANES spectra it is possible to

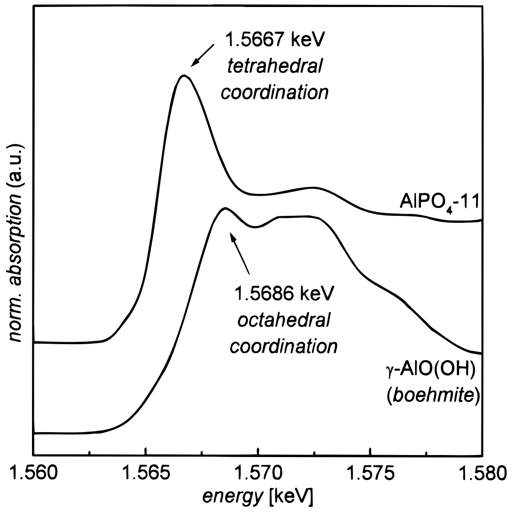

Figure 6. Al K-edge XANES spectra of microporous AlPO$_4$-11 and *boehmite*.

determine the coordination number of Al from the energy position of the K absorption edge; the exact energy of this 1s to 3p electron transition depends on the coordination number of the coordination sphere around the atom and differs by approximately 2 eV for the tetrahedral and octahedral coordination, respectively.[17,18] In aluminophosphates the Al atoms are coordinated tetrahedrally, whereas the coordination in γ-AlO(OH) (boehmite) is octahedral. However, a partial 6-fold coordination of Al in the samples may also be explained by coordination of Al with four phosphate groups and, additionally, two water molecules. Figure 6 shows the XANES spectra of a sample of crystalline microporous AlPO$_4$-11, the structure of which was verified by powder XRD, and γ-AlO(OH) (boehmite) prepared by hydrothermal treatment of Al(O^{i}Pr)$_3$ under the same conditions as for the syntheses of the mesostructured samples. The energy position of the absorption peak is characteristic of the number of oxygen atoms in the coordination shell of Al; it is found at 1.5667 keV for the tetrahedral coordination in AlPO$_4$-11 and at 1.5686 keV for the octahedral coordination in boehmite. In the following, these spectra will serve as references with respect to the energy position of the absorption edge. Figures 7 and 8 show the XANES spectra of the samples listed in Table 2.

All of the samples turn out to contain both tetrahedrally and octahedrally coordinated Al, which proves that phosphate definitely takes part in the condensation process; the mesostructured product may not be regarded as pure boehmite or any other species in which Al is exclusively octahedrally coordinated.

Furthermore, the XANES spectra allow for a quantitative determination of the relative amounts of tetrahedrally and octahedrally coordinated Al. This is demonstrated in Figure 9 for the Al K-edge spectrum of the sample B10 as an example: The spectrum contains two strongly overlapping peaks corresponding to tetrahedral and octahedral coordination, respectively.

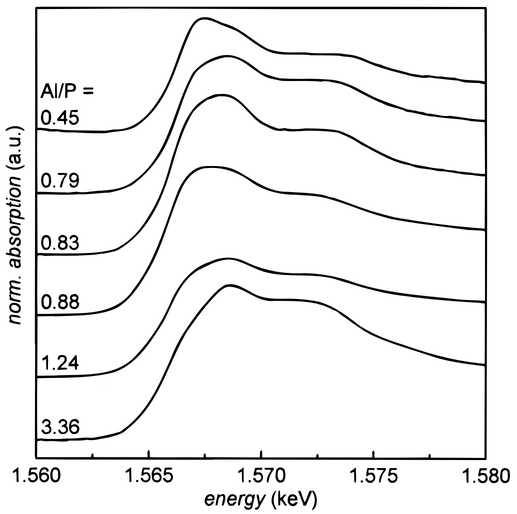

Figure 7. Al K-edge XANES spectra of samples prepared by method A with variable relative amounts of Al(O^{i}Pr)$_3$, H$_3$PO$_4$, and C$_{12}$−PO$_4$ surfactant. The relative ratios Al to overall-P as found by elemental analysis are indicated.

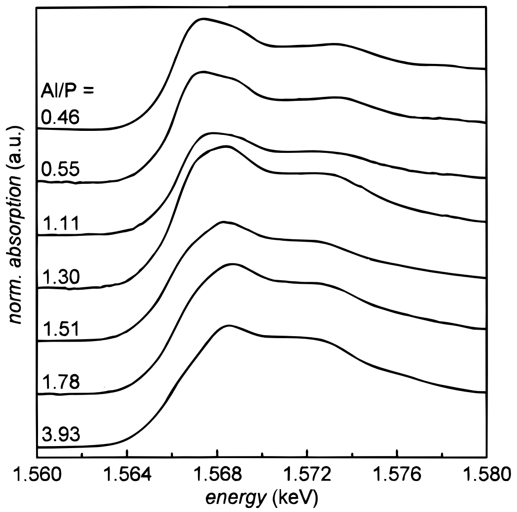

Figure 8. Al K-edge XANES spectra of samples prepared by method B with variable relative amounts of Al(O^{i}Pr)$_3$ and C$_{12}$−PO$_4$ surfactant. The relative ratios Al/P as found by elemental analysis are indicated.

This becomes apparent from the second derivative of the smoothed data (by the Savitzky−Golay method),[19,20] which features two peaks with minima at 1.5669 and 1.5689 keV, respectively. Integration of the second derivative between the roots at each peak's right and left flanks provides the areas under these peaks, the relative ratio of which (here: 0.87/0.13) corresponds to the relative ratio of tetrahedrally and octahedrally coordinated Al in the sample.

Figure 10 shows the relative amounts of tetrahedral Al in the samples as a function of the Al/P ratio found by elemental analysis. For all samples (prepared both with and without H$_3$PO$_4$) a clear correlation of the relative amount of tetrahedral Al with the Al/P ratio is observed. The tetrahedral coordination is favored if the amount of Al is about to be equal to or lower than that of P. The more Al that is present in the samples, the greater the relative amount of octahedral Al.

---

(17) Fröba, M.; Wong, J.; Rowen, M.; Brown, G. E.; Tanaka, T. Rek, Z. *Physica B* **1995**, *208 & 209*, 555

(18) Wong, J.; Rek, Z. U.; Rowen, M.; Tanaka, T.; Schäfers, F.; Müller, B.; George, G. N.; Pickering, I. J.; Via, G.; DeVries, B., Brown, G. E., Jr.; Fröba, M. *Physica B* **1995**, *208&209*, 220

(19) Savitzky, A. *Anal. Chem.* **1961**, *33*, 25A

(20) Savitzky, A., Golay, M. J. E. *Anal. Chem.* **1964**, *36*, 1627

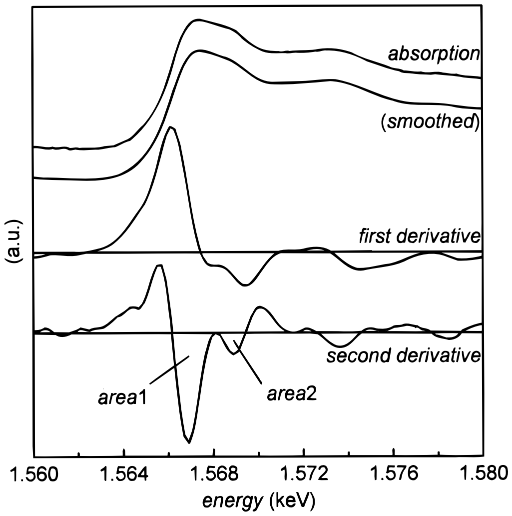

Figure 9. Example for the procedure of determining the relative amounts of tetrahedral and octahedral Al from the areas 1 and 2 under the spectrum's second derivative. Derivatives were made from the smoothed spectrum. (Sample B10)

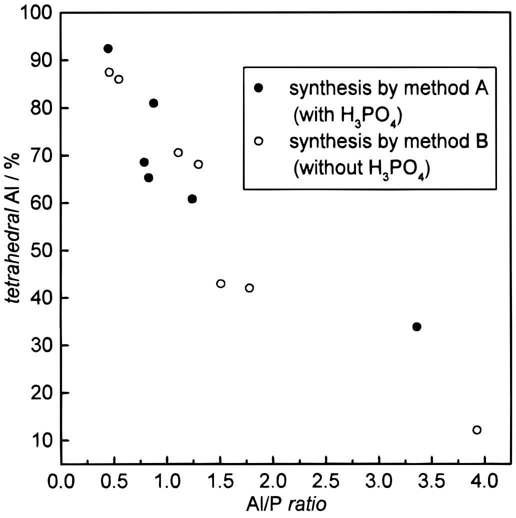

Figure 10. Relative amounts of tetrahedral Al in the samples listed in Table 2. The Al/P ratios are those found by elemental analysis.

For small amounts of Al relative to P, the presence of octahedrally coordinated Al may be explained by the coordination of two water molecules in addition to four phosphate groups, as suggested by Sayari et al.;[4] in this case the samples could be regarded as pure aluminophosphates and the Al/P ratios different from 1 would have to be accounted for by coordination sites in the Al and P tetrahedra which are not occupied by O−P or O−Al units, respectively. However, for samples with Al in a great excess relative to P, the great amounts of six-coordinated Al can hardly be attributed to coordination of water alone; thus, more or less significant amounts of an aluminum oxide or oxyhydroxide species, presumably boehmite, seem to be present in these samples, which (to a smaller degree) is probably also the case for samples which contain only small amounts of octahedral Al. Thus, for all samples it is suggested that the aluminophosphate layers contain aluminum oxide in their cores. The thickness of these oxide regions is variable and depends on the relative amounts of Al used for the synthesis.

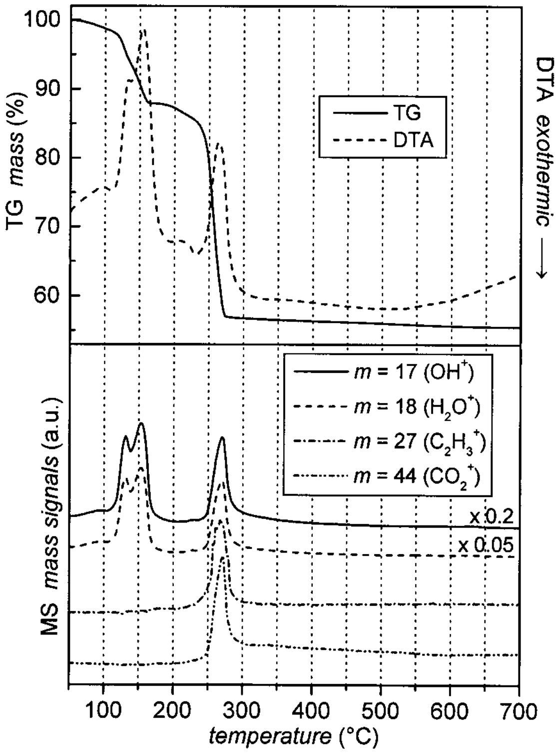

Figure 11. TG/DTA/MS diagram of the sample A3.

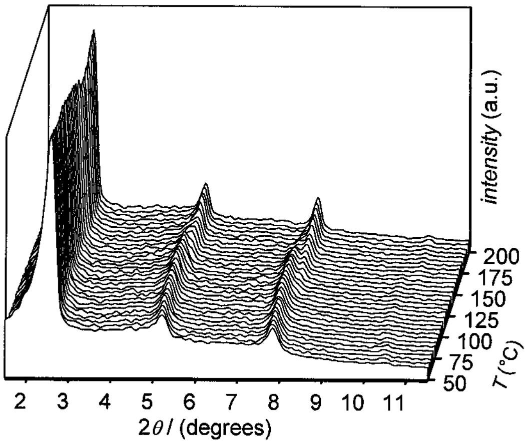

Figure 12. In-situ temperature-resolved XRD diagram of the sample A3.

Thermal Analysis. The TG/DTA/MS diagram of the sample A3 [prepared with equal amounts of $Al(O^iPr)_3$, H_3PO_4, and surfactant (5 wt %)], which is representative of the diagrams of comparable samples, is shown in Figure 11. A mass loss of 43% is observed which occurs in two relatively sharp steps, both of which are endothermic. The first one (12% loss, 120−160 °C) is attributable to the removal of water, which is intercalated between the inorganic layers; only water fragments are detected. (This process occurs in two consecutive overlapping steps.) This loss of water molecules from the interlayer regions results in a slightly closer distance between the layers, as can be monitored by in situ temperature-resolved powder XRD (Figure 12), which shows a very slight shift in the 00*l* reflections in this temperature region: The intensity of the original reflections becomes weaker with increasing temperature. Simultaneously, a new lamellar phase with smaller *d* spacing emerges, which, over a temperature interval of

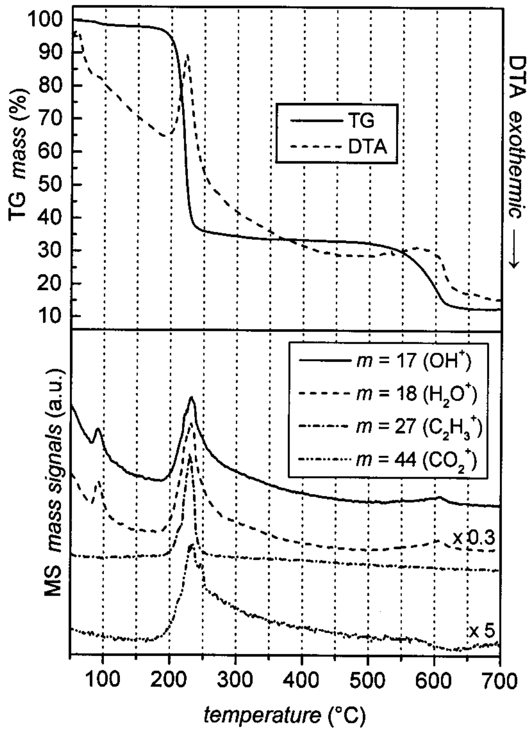

Figure 13. TG/DTA/MS diagram of C_{12}–PO_4 surfactant.

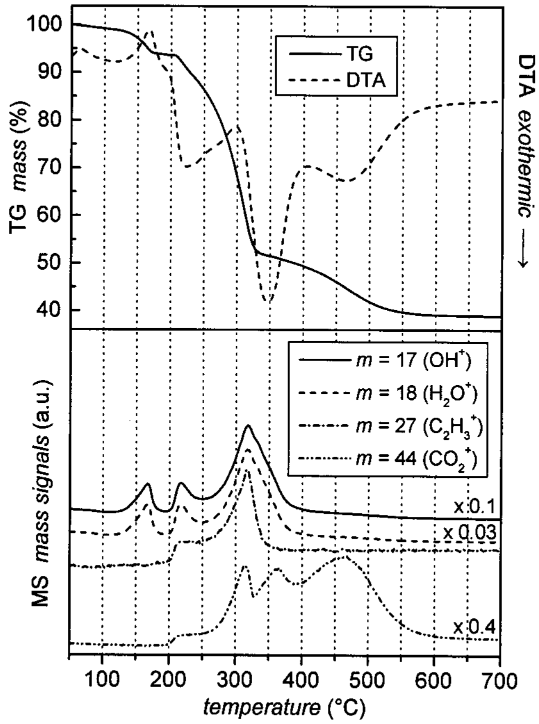

Figure 14. TG/DTA/MS diagram of the single-phase sample B3.

ca. 120–160 °C, coexists with the original one and gradually replaces it. In the second step of mass decrease (31% loss, 240–270 °C) water, ethyl, and carbon dioxide fragments are detected, corresponding to the decomposition of the surfactant molecules in the interlayer region. At higher temperatures no further mass change occurs; the final decomposition residue is X-ray amorphous.

This thermal behavior is similar to that of the pure C_{12}–PO_4 surfactant (Figure 13), where a sharp endothermic mass loss of 62%, accompanied by the detection of water, ethyl, and carbon dioxide fragments, is observed at 180–220 °C; another decrease of mass occurs at a higher temperature (19% loss, 550–620 °C), but no significant amounts of the monitored mass fragments are detected. (A mass loss of less than 3% at 90–100 °C corresponds to the removal of adsorbed water.) The surfactant molecules in the aluminophosphate sample seem to be stabilized by their regular arrangement between the inorganic layers, since their decomposition emerges at a temperature ca. 50 °C higher than in the pure (molten) state (mp = 39–45 °C).

The TG/DTA/MS diagram of the single-phase sample B3 (prepared without H_3PO_4, Figure 14), which, again, is representative, reveals a clearly different picture. The mass decrease of altogether 61% extends over a broad temperature region from ca. 100 to 600 °C and may be divided into three steps. Again, the first one (6% loss, 100–170 °C) corresponds to the endothermic removal of intercalated water. The remaining two steps (42% loss at 210–330 °C and 13% loss at 330–600 °C, respectively) are accompanied by a DTA curve and mass signals of a more complex shape. Three relatively broad exothermic DTA peaks without clear association to the TG curve and the detection of water, ethyl, and carbon dioxide fragments are observed. Thus, in the sample which was prepared without H_3PO_4, the surfactant molecules are decomposed less easily than in the sample prepared with H_3PO_4; their removal requires higher temperatures and is exothermic instead of strictly endothermic. Again, the residue of the thermal analysis is X-ray amorphous.

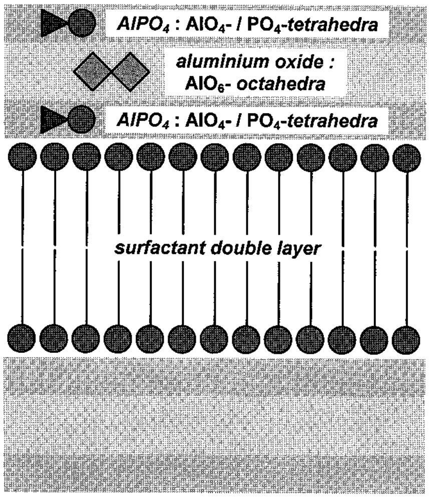

Figure 15. Schematic representation of the samples prepared with equal amounts of Al and P by method A (with H_3PO_4).

These significant differences in the thermal analyses of the samples prepared with and without H_3PO_4, respectively, are a strong indication that in the absence of H_3PO_4 the phosphate ions of the surfactant molecules are indeed incorporated into the inorganic network. On the other hand, if free phosphate ions are present, they are favored for the inorganic structure and the surfactant molecules are not covalently bonded to aluminum but form a liquid-crystal-like state between the inorganic layers. This is demonstrated schematically in Figures 15 and 16. These figures also display that the samples contain regions of aluminum oxide in the cores of the layers.

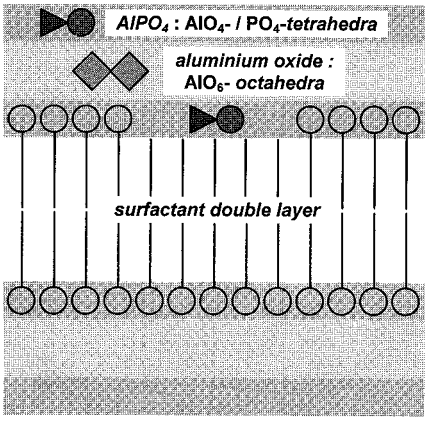

Figure 16. Schematic representation of the single-phase samples prepared with low surfactant concentrations and with equal amounts of Al and P by method B (without H_3PO_4).

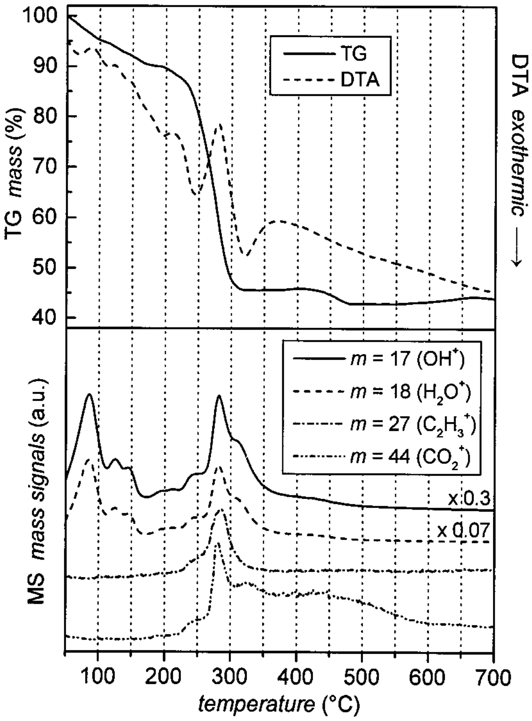

Figure 17. TG/DTA/MS diagram of the double-phase sample B6.

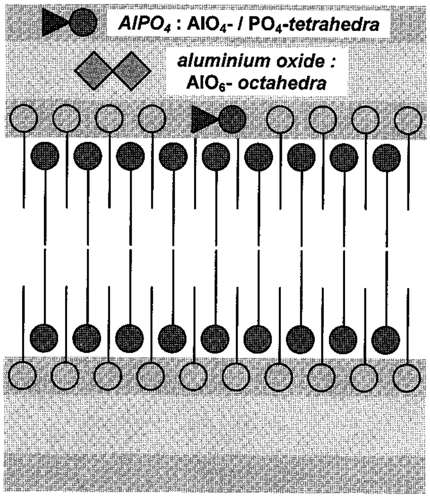

Figure 18. Schematic representation of the second phase (with larger *d* spacing) of the double-phase samples prepared with high surfactant concentrations and with equal amounts of Al and P by method B (without H_3PO_4).

In view of this model (the surfactant headgroups becoming part of the inorganic network as long as no free phosphate ions are available), why samples prepared by method A (with H_3PO_4) with a great excess of Al relative to P exhibit the smaller *d* spacing rather than the larger one must be explained: Apparently, if free phosphate ions are in relative deficiency with respect to Al, additional phosphate groups (i.e. those from the surfactant) are incorporated into the inorganic layers. This also indicates that the composition of the inorganic structure in the regions near the boundaries to the surfactant bilayers may definitely be regarded as real aluminophosphate and that aluminum oxide species, if present, are rather to be found in the core regions of the layers.

Finally, the thermal behavior of a second (representative) sample prepared without H_3PO_4 (B6) is investigated (Figure 17). This sample was prepared with a higher surfactant concentration (13 wt %) and consists of two phases; the dominant of these two phases has a larger *d* spacing (see Figure 3). The TG/DTA/MS diagram resembles both that of the sample prepared with H_3PO_4 (and, accordingly, of the pure surfactant) and that of the single-phase sample prepared without H_3PO_4. The total mass decrease of 57% is almost complete at ca 310 °C (52% loss), but occurs within a broader temperature region than in the sample prepared with H_3PO_4. Also, the DTA shows both endothermic and exothermic peaks rather than merely endothermic peaks. The loss of another 5% takes place between ca. 310 and 600 °C, accompanied by the detection of carbon dioxide. The thermal similarities of the mixture of the two phases in this sample with both other samples discussed above suggest that the two different phases originate from the two different possible roles of the surfactant phosphate groups: The phase with the smaller *d* spacing is analogous to the single-phase product obtained from the synthesis without H_3PO_4 (method B); here, the phosphate groups of the surfactant molecules are part of the inorganic layers and therefore do not contribute to the interlayer distance. The other phase with the larger *d* spacing corresponds to the situation where the surfactant headgroups are not part of the inorganic structure, as in all products prepared by method A; accordingly, the interlayer distance is greater. Apparently, the higher surfactant concentration results in an excess of surfactant phosphate groups with respect to the available Al building blocks; thus, some of the surfactant molecules can only act as template instead of becoming part of the inorganic layers, as schematically demonstrated in Figure 18. Actually, the occurrence of two lamellar phases in products obtained from syntheses with high surfactant concentrations fits in well with the proposition that the surfactant phosphate headgroups are incorporated within the inorganic layers.

Conclusions

For the first time an anionic surfactant, monododecyl phosphate, was used as a templating agent for the synthesis of mesostructured aluminophosphates. The hydrothermal synthesis leads to lamellar products that show two significant properties: (i) The samples contain variable amounts of aluminum oxide in the inner regions of the lamellae, i.e., part of the aluminum is coordinated by six oxygen atoms, as thermodynamically favored; the relative amount of six-coordinated aluminum depends systematically on the relative amounts of Al with respect to P used for the synthesis. This was demonstrated using a new method to quantitatively determine the relative degrees of different coordination behavior by Al K-edge XANES spectroscopy. (ii) As long as no free phosphate ions are offered for the condensation process, the phosphate headgroups of the surfactant become incorporated into the inorganic layers; thus, the surfactant serves both as template and as reactant. This could be derived from significant differences between samples prepared with and without H_3PO_4; these differences include *d* spacing and thermal behavior. In our opinion, a surfactant with a headgroup that can be incorporated into the inorganic network gives way to mesostructured model compounds that are of great value for further investigations. The use of monododecyl phosphate makes free phosphate ions redundant for the synthesis of mesostructured aluminophosphates; by reducing the number of interacting species by this one reactant, the system becomes easier to investigate. Thus, new opportunities in the study of the formation processes of mesostructured materials arise.

Acknowledgment. We thank Prof. Armin Reller for continuous support. The work at SSRL was supported by a generous travel grant provided by the Deutscher Akademischer Austauschdienst (DAAD) and the National Science Foundation (NSF). We are grateful to SSRL for allocating beamtime and to Dr. Joe Wong for assistance during the XAFS experiments. We also thank the members of the staff at SSRL for their support during beamtime. Financial support by the University of Hamburg, the Swiss Federal Energy Agency, the Deutsche Forschungsgemeinschaft (Fr1372/1-1), the Fonds der Chemischen Industrie, and the Werner-Ranz-Stiftung is gratefully acknowledged. We are indebted to Prof. Hans Lechert for providing the $AlPO_4$-11 reference sample. We thank Philips for the access to in situ temperature-resolved powder XRD.

CM980712C